A Kendl et al.

Interchange Instability and Transport in Matter-Antimatter Plasmas.

Interchange instability and transport
in matter-antimatter plasmas

Alexander Kendl, Gregor Danler, Matthias Wiesenberger, Markus Held

Institut für Ionenphysik und Angewandte Physik,

Universität Innsbruck, Technikerstr. 25, 6020 Innsbruck, Austria

Abstract

Symmetric electron-positron plasmas in inhomogeneous magnetic fields are intrinsically subject to interchange instability and transport. Scaling relations for the propagation velocity of density "blob" perturbations relevant to transport in isothermal magnetically confined electron-positron plasmas are deduced, including damping effects when Debye lengths are large compared to Larmor radii. The relations are verified by nonlinear full-F gyrofluid computations. Results are in favour of sufficient magnetic confinement for planned electron-positron plasma experiments. The model is generalised to other matter-antimatter plasmas. Magnetised electron-positron-proton-antiproton plasmas are susceptible to interchange driven local matter-antimatter separation, which can be expected to impede (so far unrealised) sustained laboratory magnetic confinement.

For reasons as yet elusive we are living in a world of ordinary matter only. Antimatter, predicted by Dirac less than a century ago [1], has so far made its earthly appearance through cosmic and laboratory high energy events only in exiguous quantities [2] or rather brief periods [3] before annihilating again. Macroscopic amounts of mixed matter-antimatter in the form of relativistic electron-positron pair plasmas are presumed to exist at highest energy density astrophysical objects, such as active galactic nuclei, pulsars and black holes [4].

Extended confinement of larger numbers than a few antimatter particles in the laboratory is impeded by instant annihilation at contact with materials. Ion and atom traps have been used to confine clouds of positrons or antihydrogen [5, 6]. Investigation of many-body antimatter physics on long time scales and low densities should be feasible in magnetically confined quasineutral systems of charged particles [7–9]. Generation of high-density matter-antimatter plasmas on short time scales could be achieved by laser-target interaction [3].

The most basic matter-antimatter system conceivable in the laboratory is a classical plasma with equal amounts of electrons and positrons. An electron-positron (e-p) pair plasma is a unique many-body system and distinct from a classical electron-ion (e-i) plasma in its intrinsic mass symmetry. Many fundamental instabilities that are abundant in mass-asymmetric e-i plasmas are absent in corresponding e-p systems [7]. Micro-instabilities like drift waves in inhomogeneous magnetised e-i plasmas generically result in turbulence and associated transport losses across the confining magnetic field [10]. The absence or weakness of instabilities and turbulence is consequently crucial for the quality of planned magnetically confined e-p plasma laboratory experiments [8].

Classical resistive drift wave instabilities, which rely on asymmetry in the motion of light electrons and heavier ions parallel to the magnetic field $\mathbf{B}$ with electron to ion mass ratio $m_e/m_i \ll 1$, are non-existent in e-p plasmas. Magnetic curvature induced drift-interchange modes driven by an electron or positron temperature gradient have been shown to be suppressed for e-p plasma densities N_e much smaller than the Brillouin density $N_B = \epsilon_0 B^2/(2m_e)$ by an effective screening of electric potential fluctuations on scales smaller than the Debye length [8, 11, 12]. Cross-field pressure driven interchange motion and instability of plasma perturbations is not only achievable in the presence of temperature gradients, but also for isothermal plasmas in the presence of a density gradient. Local field-aligned density perturbations with a positive amplitude, often termed "blobs", can be pushed across

the magnetic field (down the field gradient) by their own intrinsic density inhomogeneity, even for constant (flat) background density [13, 14], similar to the Rayleigh-Taylor fluid interchange instability in a gravitational field [15].

Here we show that density blobs are unstable in an inhomogeneously magnetised e-p plasma for a range of accessible parameters and thus can lead to crucial transport losses. We present a simple relation to estimate the critical parameters for Debye stabilisation of e-p blob propagation, which we verify by nonlinear full-F gyrofluid computations.

In addition to e-p pair plasmas we also consider more general matter-antimatter plasmas. When the Debye length is much smaller than the drift scale, e-p plasmas preserve quasi-neutrality and thus local equality of the electron and positron number densities $N_e(\mathbf{x}, t) = N_p(\mathbf{x}, t)$ under the influence of the drift-interchange instability. For quasi-neutral matter-antimatter ambi-plasmas consisting of initially equal electron, proton, positron and antiproton densities (which could in some future experiment be feasible, but is cosmologically probably irrelevant) we show that such a (quasi-neutral) one-to-one correspondence of matter and antimatter particle densities is no longer maintained: the ambi-plasma interchange instability does not only lead to transport but also to spatial matter-antimatter separation.

First, we analyse magnetised e-p plasmas by means of a full-F gyrofluid model [16], which is derived from a gyrokinetic model that evolves the full distribution function $F(\mathbf{x}, \mathbf{v}, t)$. In the isothermal two-dimensional limit [17, 20] the model consists of continuity equations for the gyrocenter densities n_s for electron and positron species $s \in (e, p)$,

$$\partial_t n_s = \frac{1}{B} [n_s, \psi_s] + n_s \hat{\kappa}(\psi_s) + \tau_s \hat{\kappa}(n_s), \tag{1}$$

coupled by polarisation to the electric potential ϕ in Poisson's equation:

$$\sum_s Z_s N_s + \varepsilon \, \nabla_\perp^2 \phi = 0. \tag{2}$$

Exact local quasi-neutrality is thus violated for $\varepsilon \neq 0$. The particle densities N_s with charge states $Z_e = -1$, $Z_p = +1$ are linked to the gyrocenter densities n_s via

$$N_s = \Gamma_{1s} n_s + \boldsymbol{\nabla} \cdot \left(n_s \frac{\mu_s}{Z_s B^2} \boldsymbol{\nabla}_\perp \phi \right). \tag{3}$$

In contrast to strictly quasineutral e-i gyrofluid systems as in ref. [16], we do not invoke

3

the gyrokinetic ordering ($\varepsilon \ll 1$), but retain in our present e-p model the Debye parameter

$$\varepsilon = \left(\frac{\lambda}{\rho}\right)^2 = \frac{2N_B}{N_{e0}}, \tag{4}$$

which represents effects of finite Debye length $\lambda = \sqrt{\epsilon_0 T_e/(e^2 N_{e0})}$ in relation to the Larmor radius $\rho = \sqrt{T_e m_e}/(eB_0)$. Here T_e is the electron temperature, m_e the electron mass, and B_0 a reference magnetic field strength. The temperature ratio is $\tau_s = T_s/(Z_s T_e)$ so that $\tau_e = -1$ and $\tau_p \geq 0$. The e-p mass ratios $\mu_s = m_s/m_p = 1$ are both unity so that $\mu \equiv \sum_s \mu_s = \mu_e + \mu_p = 2$, in contrast to e-i plasmas where $\mu = \mu_e + \mu_i \approx \mu_i = 1$. Annihilation between positrons and electrons is here neglected for the time scales of blob propagation [21].

Finite Larmor radius and ponderomotive effects enter via $\psi_s = \Gamma_{1s}\phi - (1/2)(\mu_s/Z_s B^2)(\nabla_\perp \phi)^2$. The gyro-averaging operator in Padé approximation is defined by $\Gamma_{1s} = (1 + (1/2)b_s)^{-1}$ with $b_s = -(\mu_s \tau_s/Z_s)\nabla_\perp^2 = k_\perp^2$ here. The gyrocenter densities n_s have been normalised to a constant reference density n_0, so that the magnitude of the plasma density $n_s \leftarrow n_s/n_0$ is of order one, and the potential is normalised to $\phi \leftarrow (e\phi/T_e)$. Perpendicular scales and spatial derivative operators are normalised to the drift scale ρ so that $\nabla \leftarrow \rho\nabla$. The time scale is normalised as $\partial_t \leftarrow (\rho/c_s)\partial_t$ with sound speed $c_s = \sqrt{T_e/m_e}$. The 2-d advection terms are expressed through Poisson brackets $[f, g] = (\partial_x f)(\partial_y g) - (\partial_y f)(\partial_x g)$ for local coordinates x and y perpendicular to $\mathbf{e}_z = \mathbf{B}/|B|$. Normal magnetic curvature $\kappa = \partial_x \ln B \equiv 2\rho/R$ (including magnetic curvature and gradient drifts) enters into $\hat{\kappa} = \kappa \, \partial_y$. For most toroidal magnetic confinement experiments the gyro scale ρ is much smaller than the effective curvature radius R, which can be well approximated by the torus radius, so that $\kappa \ll 1$.

We analyse the dependence of the ideal interchange growth rate on the Debye screening parameter ε in the present model by linearising eqs. (1) and (2) on top of a background density $n_0(\mathbf{x})$ for small perturbation amplitudes proportional to $\tilde{n}_e, \tilde{n}_p, \tilde{\phi} \sim \exp(-i\omega t + i\mathbf{k} \cdot \mathbf{x})$ and small curvature. For simplicity we neglect finite Larmor radius effects in the analytical treatment and set $b_s = 0$. We get the linear system of equations, with $s \in (e, p)$:

$$-\omega \tilde{n}_s = (\omega_c - \omega_*)\tilde{\phi} + \tau_s \omega_c \tilde{n}_s, \tag{5}$$

$$(\mu + \varepsilon)k_\perp^2 \tilde{\phi} = \tilde{n}_p - \tilde{n}_e. \tag{6}$$

Here $\omega_c = \kappa k_y$ and $\omega_* = -g k_y$, with $g = \partial_x \ln n = -L_n^{-1}$ for a constant density gradient

length L_n, where $g = g_0 + g_1$ is composed of a background gradient g_0 and a contribution g_1 by the intrinsic blob front. The linearisation of the Poisson equation resembles a Boussinesq approximation. The system is easily resolved into a dispersion relation $\omega = \omega(\mathbf{k}, \varepsilon)$. For $\omega = \omega_r + i\gamma$ we obtain an interchange growth rate γ with

$$\gamma^2 = \frac{1 + \tau}{\mu + \epsilon} \left[\frac{\omega_c}{k_\perp^2}(\omega_* - \omega_c) - \frac{1}{4}(\mu + \epsilon)(1 + \tau)\omega_c^2 \right]. \tag{7}$$

The model is interchange unstable for $\gamma^2 > 0$. Here for e-p plasmas $\mu = 2$ (with $\tau \equiv \tau_p$ and $\tau_e = -1$), whereas for quasineutral e-i plasmas we would have $\mu = 1$ and $\epsilon = 0$.

We apply the blob correspondence principle [13] which assumes that the perturbation mode most relevant for instability of the blob front and thus for the resulting blob propagation is of the actual initial blob scale σ. For Gaussian blobs with width σ, which relates $k_y = k_x \approx 1/\sigma$ and $k_\perp^2 = k_x^2 + k_y^2 \approx 2/\sigma^2$. Relating the growth rate to blob convection by $i\gamma \sim (d/dt) \sim v_x \partial_x \sim iv_x/\sigma$, the blob propagation velocity can be approximated as $v_x = \sigma\gamma$.

We here neglect a background gradient so that $g_0 = 0$, and $g_1 = \partial_x \ln n \approx (1/n_0)\partial_x n$ is evaluated for an initial Gaussian blob density $n(\mathbf{x}) = n_0 + A\exp(-\mathbf{x}^2/\sigma^2)$ at the location $x = \sigma/\sqrt{2}$ of the steepest front gradient to be $g_1 = -\sqrt{(2/e)} \cdot A/\sigma \equiv -a/\sigma$ with $a \approx 0.86A$.

In the following we set $\tau = \tau_p = 1$, $\mu = 2$. In the blob correspondence principle approximation we thus obtain

$$v_x = \frac{1}{\sqrt{1 + (\varepsilon/2)}} \sqrt{\frac{1}{2}a\kappa\sigma - \kappa^2\sigma^2 \left[\frac{1}{2} + \frac{1 + (\varepsilon/2)}{\sigma^2} \right]}. \tag{8}$$

For $\kappa\sigma \ll 1$ the second term can be neglected (except for very large ε or very small amplitudes) so that the e-p blob velocity can be approximated as

$$v_{x0}(\varepsilon) \approx \frac{v_0}{\sqrt{1 + (\varepsilon/2)}} \quad \text{with} \quad v_0 = \sqrt{0.43\,A\kappa\sigma}. \tag{9}$$

We verify the (range of) validity for the relations in eqs. (8) and (9) by numerical simulation of blob propagation for various parameters in the full-F nonlinear model eqs. (1, 2) using the codes TOEFL [19, 20] and FELTOR [17, 18]. During its propagation down the magnetic field gradient the unstable blob changes its shape in the simulations from initially circular $O \rightarrow D \rightarrow \supset$ to mushroom cap shape, with subsequent vortex roll-up and final turbulent break-up. Typical density structures of the rightward propagating blob at three different times for $\varepsilon = 0$ (top) and $\varepsilon = 50$ (bottom) are shown in Fig. 1 for an amplitude $A = 0.5$, width $\sigma = 10$ in units of ρ, and curvature $\kappa = 10^{-4}$. The computational domain is $(128\,\rho)^2$
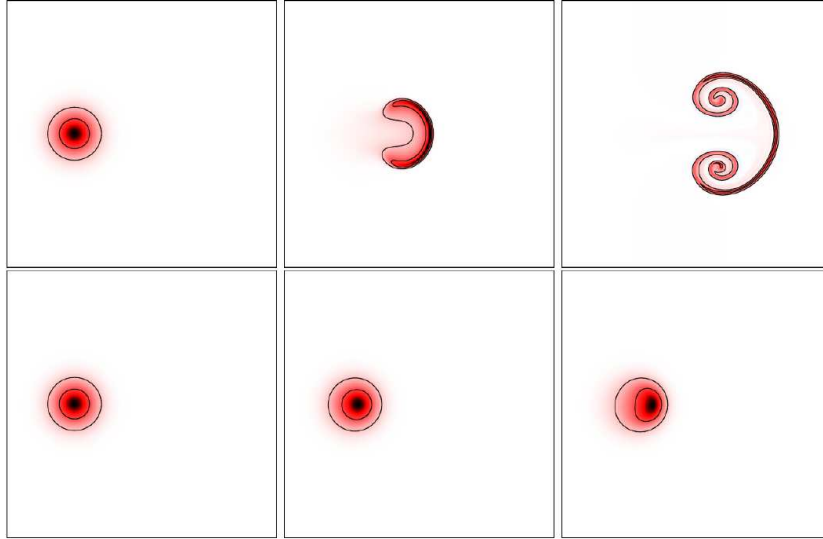
FIG. 1: *Interchange driven propagation of an initially Gaussian density perturbation in an inhomogeneous magnetic field: comparison between exactly quasi-neutral plasma with $\varepsilon = 0$ (top row) to Debye screened plasma with $\varepsilon = (\lambda/\rho)^2 = 50$ (bottom row), shown at three times (from left to right: $t = 0$, $t = 25000$, $t = 50000$ in units of ρ/c_s). The colour scale indicates positive blob density compared to the background ($n_0 = 1$), with contour lines drawn at $n = 1.1$ and $n = 1.3$.*

with a grid resolution of 512^2. The simulation illustrates that blob transport is for these parameters strongly inhibited by Debye screening with $\varepsilon = 50$ (bottom).

We compare the analytical propagation velocity estimates v_x with the maximum center-of-mass velocity $v_{sim} \equiv \max(v_{com})$ in the blob simulations, where $v_{com} \equiv \dot{x}_{com}$ with $x_{com} \equiv [\int dxdy(n_e(x,y) - n_0)x]/[(\int dxdy(n_e(x,y) - n_0)]$ for mass symmetric e-p plasmas. The maximum velocity, which coincides for gyrocenter and particle densities, is usually obtained in the bean ("D") shaped phase.

In Fig. 2, $v_{sim}(\varepsilon)$ computed from the full model simulation (symbols), and the corresponding analytical estimates $v_x(\varepsilon)$ from eq. (9) (continuous curves) are plotted as a function of Debye screening ε for various blob parameters. In all cases the velocities qualitatively correspond well to the scaling $v_{x0}(\varepsilon) = v_0/\sqrt{1 + (\varepsilon/2)}$ over several orders of magnitude. The four cases shown here are: $A = 0.5$, $\sigma = 10$ (black/circles); $A = 0.1$, $\sigma = 100$ (blue/stars); $A = 0.05$, $\sigma = 40$ (green/diamonds); $A = 0.05$, $\sigma = 10$ (red/squares). The curvature parameter is $\kappa = 10^{-4}$. Simulation domain sizes are adapted to ensure at least $L_y > 10\sigma$
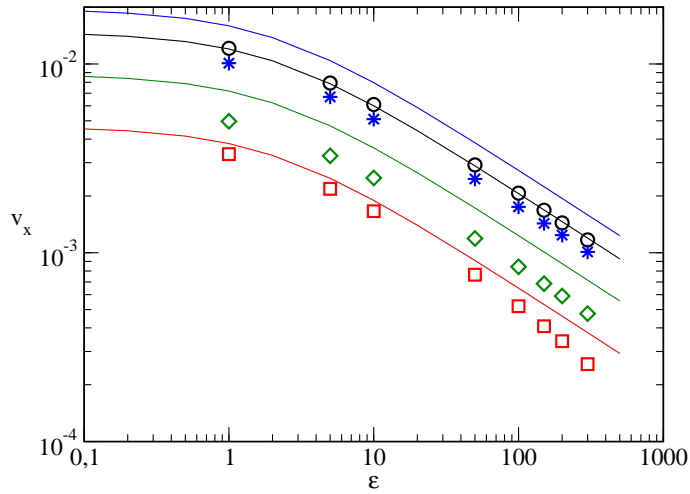
FIG. 2: *Scaling of simulated maximum electron-positron blob velocities v_{sim} (symbols) and theoretical velocity scaling v_x (curves) with Debye screening parameter ε. For all blob parameters the velocities qualitatively follow the scaling $v_{x0}(\varepsilon) = v_0/\sqrt{1 + (\varepsilon/2)}$ over several orders of magnitude. Black/circles: $A = 0.5$, $\sigma = 10$; blue/stars: $A = 0.1$, $\sigma = 100$; green/diamonds: $A = 0.05$, $\sigma = 40$; red/squares: $A = 0.05$, $\sigma = 10$. Quantitative agreement of simulations with the analytical scaling law is achieved only for large blob amplitudes and/or small blob widths (e.g. here the case shown in black, less for red).*

in order to minimise boundary effects. Quantitative agreement between the linear scaling law (curves) and simulations is best achieved for large blob amplitudes and/or small blob widths (i.e. the cases shown in red and black). The largest quantitative differences between analytical estimate and simulations appear for the cases with small amplitudes and large blob sizes (shown here in blue and green), which is in agreement with an e-i scaling law based on energetic principles [23]. A noticeable qualitative deviation is observed in the (red) case with both small amplitude and small blob width for large ε: in connection with the slow propagation velocity (and longer simulation time), numerical viscosity and diffusion effects can in this case play a larger role. The blob propagation velocities drop by more than an order of magnitude for $\varepsilon > 200$.

In experiments with magnetically confined e-p plasmas the interchange driven transport of blob-like random density fluctuations is consequently effectively reduced if large values of ε can be achieved. For the projected APEX electron-positron stellarator experiment [9] the

major torus radius is $R = 15$ cm, and planned plasma temperatures are in the order of 0.2 - 2 eV at a magnetic field strength of $B = 2$ T. This results in an electron/positron gyro radius of $\rho \sim 10^{-3}$ cm. Foreseen particle densities are around 10^{13} m^{-3}, which results in Debye lengths $\lambda \sim 0.1 - 0.3$ cm [9]. The curvature parameter thus is in the order of $\kappa \sim 10^{-4}$ and the Debye parameter is expected around $\varepsilon \sim 50 - 300$. An unknown quantity in the estimations of interchange driven transport is the size and amplitude of appearing density perturbations. In e-i tokamak edge plasmas the observed blob structures are generated by drift wave vortices or are sheared off by perpendicular flows, which results in typical sizes in the order of a few to 20 (ion) drift scales. Blob and vortex amplitudes in the tokamak edge are found in the range around $A \sim 0.01 - 1$ relative to background densities. For magnetically confined e-p plasmas we can not assume the same parameters for initial seed perturbations, as driving by drift wave vortices is absent, and the possible flow shearing rate is unknown. But as the e-p plasma is not exactly quasi-neutral, small local electric field or density perturbations can appear spontaneously with cross-field extensions up to the order of the Debye length. It therefore appears appropriate to consider blob sizes in the order between $\sigma \sim 1 - 200$, with a wide range of possible initial perturbation amplitudes (as for the computations in Fig. 2). We stress that an additional background density gradient (which is expected in any magnetically confined plasma) will add to the interchange driving rate.

We now discuss parameters required for complete stabilisation of e-p blobs. As can be seen from eqs. (7) and (8), the system is stable for $\varepsilon = 0$ when $(0.43A\kappa\sigma - 0.5\kappa^2\sigma^2 - \kappa^2) < 0$. This is achieved for blob amplitudes less than $A_{crit} = 1.16\kappa\sigma$. Here we are more interested in the stability criterion for finite Debye parameter ε, which leads to a minimum ε for stabilisation:

$$\varepsilon \geq \sigma \left(\frac{a}{\kappa} - \sigma \right) - 2 \approx \sigma^2 \left(\frac{a}{\kappa\sigma} - 1 \right). \tag{10}$$

For $\sigma = 10$, $\kappa = 10^{-4}$ and $A = 0.01$ this corresponds to $\varepsilon_{crit} \approx 700$. For larger amplitudes the limit is higher. This blob stabilisation is also observed in simulations. For example, $\varepsilon \approx 300$ is expected in the planned APEX experiment [9]. This would not be sufficient to completely stabilise self-propelled interchange blobs of sizes in a wide range of relevant parameters by Debye screening, but particle transport $\Gamma \sim Av_x \sim 1/\sqrt{1 + (\varepsilon/2)}$ would nevertheless be significantly reduced by around an order of magnitude (compared to $\varepsilon = 0$). In order to maintain large $\varepsilon = (\lambda/\rho)^2 = (2N_B/N_{e0})$ in e-p experiments, the particle densities have to be

kept at sufficiently small values $N_{e0} \ll N_B = \epsilon_0 B^2/(2m_e)$.

In addition to the self-propelled blobs which require finite amplitude, the linear analysis also shows interchange instability for arbitrary small perturbations on an additional large enough background density gradient. But as both the perturbation amplitudes and widths to be expected in an e-p plasma are largely unknown, prediction of the actual quantitative level of convective interchange driven transport in toroidal magnetically confined e-p plasmas is difficult. As an order of magnitude estimate for cross-field transport in the APEX experiment ($N \sim 10^{13}$ m^{-3}), we arrive at a radial density flux $\Gamma = (AN)(v_x c_s) \approx (0.01 \cdot 10^{13}$ m$^{-3}) \cdot (0.01 \cdot 10^5$ m s$^{-1}) \approx 10^{14}$ m^{-2} s^{-1}. For an APEX scale plasma surface $S \sim 0.1$ m^2 this would correspond to a loss rate of 10^{13} particles per second and a consequent confinement time of milliseconds to seconds, depending crucially on the possible fluctuation amplitudes and scales, which should (in the absence of other instabilities) be given by the thermal background fluctuation level. Our results on self-propelled or density gradient driven blob transport complement the discussion of temperature gradient driven instabilities in e-p plasmas in refs. [8, 11, 12] and to some extent confirm the optimistic confinement expectations for the APEX experiment [9].

The apparent prospect of creating macroscopic magnetically confined electron-positron plasmas in the laboratory motivates to consider other possible many-body matter-antimatter systems. From symmetry principles, it appears attractive to study a quasi-neutral system consisting of equal numbers of electrons, protons, positrons and antiprotons. It is unclear and, regarding present standard models of baryogenesis and magnetogenesis, highly unlikely, whether such a magnetised "ambi-plasma" (following a terminology introduced by Hannes Alfvén) has actually ever existed in cosmological history, but it might in principle be created in laboratory when large numbers of positrons and antiprotons could be supplied continuously at one site (cf. ref. [2]).

We therefore briefly complement the discussion of our results presented above by computations of quasi-neutral density blob perturbations in such an ambi-plasma. The model is again given by eqs. (1), (2) and (3) with $s \in (e, i, p, a)$ consisting of electrons, ions (protons), positrons and antiprotons. All scales are now normalised to the proton drift scale $\rho = \sqrt{T_e m_i}/(eB)$, and Debye screening is neglected ($\varepsilon = 0$). We initialise with a matter-antimatter symmetric Gaussian density perturbation with same parameters $n_s(\mathbf{x}) = n_0 + A \exp(-\mathbf{x}^2/\sigma^2)$ for all $s \in (e, i, p, a)$. FLR effects are now neglected for the leptons (e,
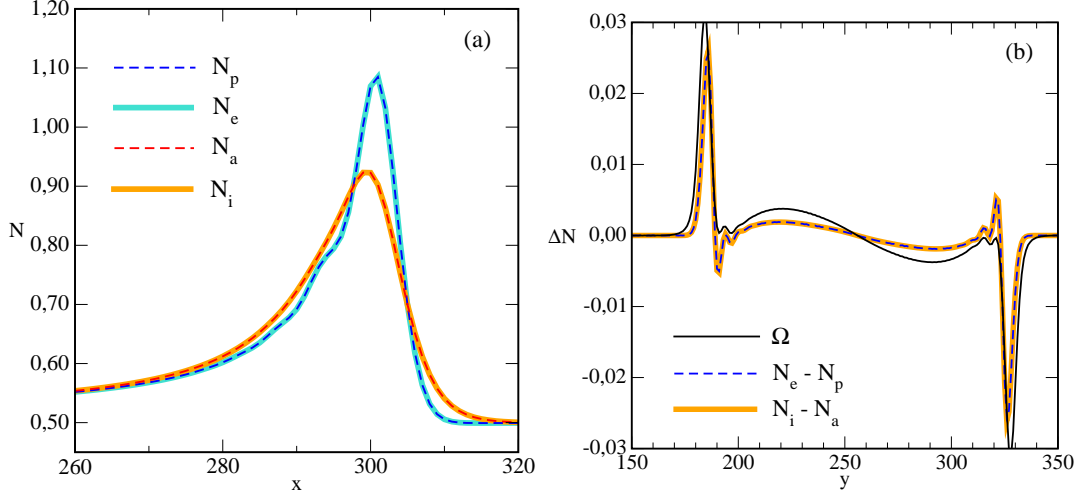
FIG. 3: *Species asymmetry in an ambi-plasma blob. (a) Cut in propagation (x) direction through blob center: electron and positron particle densities (N_e, N_p) deviate from proton and antiproton densities (N_i, N_a). (b) Cut in perpendicular (y) direction through blob center: differences in particle-antiparticle densities are correlated with the vorticity Ω. Cross-sections are plotted for a mushroom cap blob shape corresponding to the top right frame in Fig. 1.*

p), but retained for the baryons (i, a) in $\tau_i = 1$ and $\tau_a = -1$. The overall evolution of the ambi-plasma blob is at the beginning similar to the case of e-i or e-p blobs: the magnetic curvature induced interchange mechanism generates an electric dipole potential $\phi(\mathbf{x})$ with an associated vorticity field $\Omega(\mathbf{x}) = \nabla^2 \phi$ that drives the blob down the magnetic field gradient.

Remarkably, the detailed spatial matter-antimatter symmetry is partially broken during the further blob development in two ways: Fig. 3 (a) shows that the particle densities $N_s(x)$ clearly start to differ between species. The electron and positron densities are closely aligned with each other, and so, respectively, are the proton and antiproton densities: leptonic and baryonic densities locally deviate from each other.

Fig. 3 (b) reveales that also the particle-antiparticle symmetry is locally broken, where both ($N_e - N_p$) and ($N_i - N_a$) differences grow with time. The curves for the electron-positron density difference (dashed blue) exactly agree with the proton-antiproton density difference (bold orange) because of the quasineutrality condition ($\sum_s Z_s N_s = 0$). Both appear strongly correlated with the vorticity Ω.

The local baryon-lepton asymmetry in particle densities N_s is caused by finite Larmor radius (FLR) effects, which mainly enter via $N_s \sim \Gamma_{1s} n_s = n_s/(1 + (1/2)b_s)$ and reduce

10

the particle densities of the species (baryons) with relevant masses μ_s in regions of steep gradients. This asymmetry disappears when FLR effects are switched off in the simulation.

The breaking of the local particle-antiparticle symmetry is, in contrast, a result of alignment with vorticity [22] driven by the interchange instability, and consequently grows with time during the blob evolution. The asymmetry is again most pronounced at steepening blob edges. It persists when $\tau_i = \tau_a = 0$ and is thus not related to FLR effects. Taking the total time derivative of the polarisation equation (linearised, without FLR terms) we have $D_t(N_p - N_e) = D_t(N_i - N_a) \sim \hat{\kappa}(N_e + N_p) \sim (\mu_i + \mu_a)D_t\Omega$ with $\Omega = \nabla_\perp^2 \phi$.

A consequence of the particle-antiparticle asymmetry appears particularly in the presence of annihilation, which can play a stronger role on the ion blob evolution time scale (that is larger by m_i/m_e compared to e-p blob time scales), and will enhance the relative particle-antiparticle density difference. As the interchange drive is present in any inhomogeneously magnetized plasma, matter-antimatter ambi-plasmas will loose their symmetry on combined interchange and annihilation time scales, and in the worst case will result in patches of electron-proton matter locally separated from positron-antiproton antimatter plasma. This matter-antimatter separation by plasma instabilities reduces the prospect of achieving magnetic confinement of laboratory ambi-plasma.

In summary, we have shown that transport of plasma density by interchange driving appears for a large range of parameters in e-p plasmas, but can (similarly to previously discussed temperature gradient driven modes) be significantly reduced by maintaining a high enough density to facilitate damping by Debye screening. Magnetic confinement of e-p plasmas for relevant time scales so appears to be feasible. In contrast, we have further argued that long confinement of matter-antimatter ambi-plasmas consisting of globally equal numbers of electrons, protons, positrons and antiprotons is likely inhibited by local matter-antimatter separation in the presence of annihilation.

---

[1] P.A.M. Dirac. Math. Proc. Cambridge Philos. Soc. **26**, 361 (1930).

[2] The ALPHA Collaboration. Nature Physics **7**, 558 (2011).

[3] G. Sarri, K. Poder, J.M. Cole, et al. Nature Communications **6**, 6747 (2015).

[4] R. Ruffini, G. Vereshchagin, S.-S. Xue. Physics Reports **487**, 1 (2010).

[5] J. Danielson, D. Dubin, R. Greaves, and C. Surko. Rev. Mod. Phys. **87**, 247 (2015).

[6] R.G. Greaves, C.M. Surko. Phys. Plasmas **4** 1528 (1997).

[7] V. Tsytovich, C.B. Wharton. Comments Plasma Phys. Controlled Fusion **4**, 91 (1978).

[8] T.S. Pedersen, A.H. Boozer, W. Dorland, J.P. Kremer, and R. Schmitt. J. Phys. B: At. Mol. Opt. Phys. **36**, 1029 (2003).

[9] T.S. Pedersen, J.R. Danielson, C. Hugenschmidt, G. Marx, X. Sarasola, F. Schauer, L. Schweikhard, C.M. Surko, and E. Winkler. New Journal of Physics **14**, 035010 (2012).

[10] W. Horton, Rev. Mod. Phys. **71**, 735 (1999).

[11] P. Helander. Phys. Rev. Lett. **113**, 135003 (2014).

[12] P. Helander, J.W. Connor. J. Plasma Phys. **82**, 905820301 (2016).

[13] S.I. Krasheninnikov, Physics Letters A **283**, 368370 (2001).

[14] D. A. D'Ippolito, J. R. Myra, and S. J. Zweben. Phys. Plasmas **18**, 060501 (2011).

[15] O. E. Garcia, N. H. Bian, V. Naulin, et al. Physica Scripta **T122**, 104 (2006).

[16] J. Madsen, Phys. Plasmas **20**, 072301 (2013).

[17] M. Wiesenberger, J. Madsen, A. Kendl, Phys. Plasmas **21**, 092391 (2014).

[18] G. Danler, *Zur Austauschinstabilität im magnetisierten Elektron-Ion und Elektron-Positron Plasma*, MSc Thesis, 02.12.2015, Universität Innsbruck (unpublished).

[19] A. Kendl, Int. J. Mass Spectrometry **365/366**, 106 (2014).

[20] A. Kendl, Plasma Phys. Contr. Fusion **57** 045012 (2015).

[21] P. Helander, D.J. Ward. Phys. Rev. Lett. **90**, 135004 (2003).

[22] A. Kendl, Phys. Plasmas **19**, 112301 (2012).

[23] R. Kube, O.E. Garcia, M. Wiesenberger, accepted at Phys. Plasmas (2016).